NORMAL MAMMOGRAM CLASSIFICATION BASED ON REGIONAL ANALYSIS

Yajie Sun †, *Charles F. Babbs* ‡, *and Edward J. Delp* †

†Video and Image Processing Laboratory
School of Electrical and Computer Engineering
Purdue University
West Lafayette, IN 47907-1285

‡Department of Basic Medical Sciences
School of Veterinary Medicine
Purdue University
West Lafayette, IN 47907-1246

ABSTRACT

The majority of screening mammograms are normal. It will be beneficial if a detection system is designed to help radiologists readily identify normal regions of mammograms. In this paper, we will present a binary tree classifier based on the use of global features extracted from different levels of a 2-D Quincunx wavelet decomposition of normal and abnormal regional images. This classifier is then used to classify whether an entire whole-field mammogram is normal. This approach is fundamentally different from other approaches that identify a particular abnormality in that is independent of the particular type of abnormality.

1. INTRODUCTION

Breast cancer is the second-leading cause of cancer death in women after lung cancer, and it is the leading cause of cancer death among women age 35 to 54. Early detection is the most effective way to prevent death, and screening mammography is still the gold standard.

Computer-aided systems have been developed to improve radiologists' mammographic screening efforts [1]. A potential way to design a computer-aided system is to identify normal mammogram regions with very high specificity and allow radiologists to focus more on suspicious areas, since most mammograms are normal. This strategy could improve screening efficiency and true positive rate in mammographic screening. Little has been done on computer-aided normal mammogram detection, though many individual cancer detection systems have been developed in the last decade, such as speculated lesion detection [2]. In [3] a statistical modelling method for identifying normal areas from abnormal regions is presented. This approach is based on the distribution of microcalcifications and is essentially a microcalcification detector. In [4] a method of linear normal structure identification and removal for the enhancement and analysis of normal mammograms was described. In this paper, we present a normal detection scheme that classifies normal regions from suspicious regions, independent of the abnormality present.

Address all correspondence to E. J. Delp, ace@ecn.purdue.edu.
This work was supported by a grant from Qualia Computing, Inc.

2. NORMAL REGIONAL CLASSIFICATION

In this section we describe our normal regional mammogram classifier used to classify normal regions from abnormal regions [5]. Multi-resolution features are extracted from the image of regional mammograms and used to train and test a binary decision tree. The binary decision tree classifies every region of interest as either normal (N) or suspicious (S), and assigns the label N or S to the region.

2.1. Residual Images

All mammograms used in our study were selected from the Digital Database for Screening Mammography (DDSM) distributed by University of South Florida [6]. The gray level is mapped into optical density to discount the different scanner settings. A region of interest (ROI) with size 512×512 is extracted from either a normal or cancer case. Normal ROIs are extracted from normal cases; cancer ROIs are extracted from cancer cases with the cancer in the center of the ROI according to the ground-truth image. For our study 120 normal ROIs and 112 abnormal ROIs were obtained from the database. In 112 abnormal cases, 40 were identified as ill-defined or circumscribed masses, 33 were spiculated lesions and 39 were microcalcifications.

A line detection scheme, described in [7], is used to identify and remove linear structures of clinically normal tissue from the ROIs [4]. After linear structure removal, the "residual" image of the normal ROIs appear relatively featureless. For abnormal mammograms, the "residual" image consist of contrast enhanced abnormalities within a normal structure suppressed background.

0-7803-7523-8/02/$17.00 ©2002 IEEE

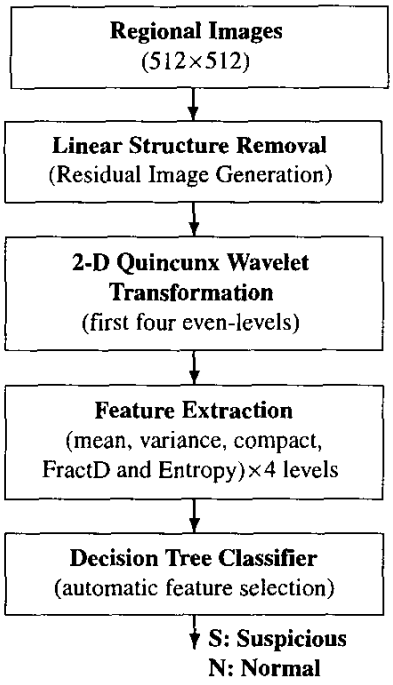

Figure 1: Diagram of normal region classifier.

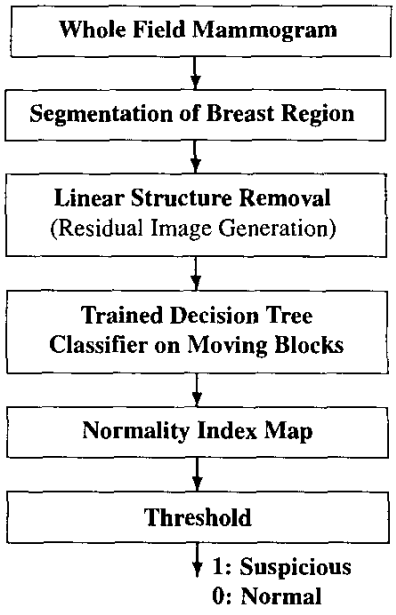

Figure 2: Diagram of Whole-Field Classification

2.2. Multi-resolution Features Extraction

The 2-D Quincunx wavelet transform described in [8] is used to obtain a multi-resolution decomposition of the "residual" images. This 2-D nonseparable transform does not introduce phase distortion in the decomposed images, and its frequency band decomposition is much closer to the human visual system than that of a 2-D separable transform. We only select the first four even-level decomposition images, i.e. images of spatial resolutions $(N/2\times N/2)$, $(N/4\times N/4)$, $(N/8\times N/8)$ and $(N/16\times N/16)$ for feature extraction assuming that the original image size is $N\times N$.

For every selected decomposition image, five features, *Mean, Variance, Compactness (compact), Fractal Dimension (FractD), and Entropy*, are extracted globally from that decomposition image. *Mean* is the average pixel value, and *Variance* is the global standard deviation of the decomposition image. *Entropy* is computed from 20-bin histogram. *Compactness* and *Fractal Dimension* are extracted from the binarized and morphologically processed decomposition image. Therefore, there are twenty features extracted from the four even-level decomposition images, which become the feature vector for the corresponding ROI. Therefore, we obtain 120 feature vectors of normal ROIs and 112 feature vectors of abnormal ROIs for the construction and testing of the decision tree classifier.

2.3. Binary Decision Tree Classifier

The binary decision tree is selected to separate normal and abnormal regions. Such a classifier incorporates automatic feature selection and complexity reduction. The binary decision tree is constructed using the convergent algorithm in [9][2], which is much faster than CART [10]. Each leaf node of the decision tree is labelled as one of two classes: S represents the class identified as suspicious, and N presents the class identified as normal. Two thirds of 120 normal and 112 abnormal feature vectors were randomly selected as the training set, and the remaining one third feature vectors were used as the test set. Therefore, the training data

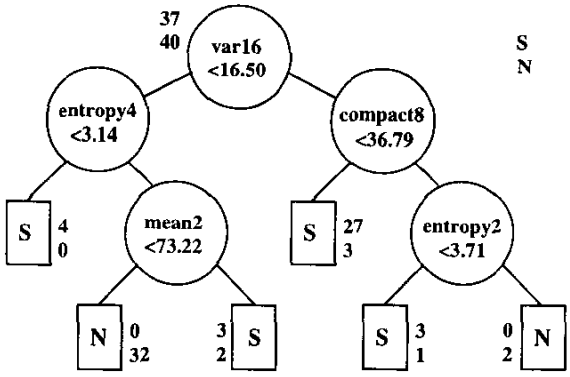

Figure 3: Trained Binary Decision Tree

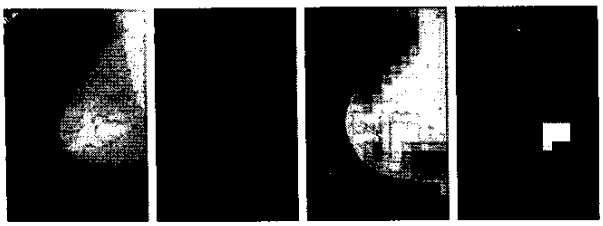

(a) (b) (c) (d)

Figure 4: (a) Whole-Field Mammogram, (b) Residual Image, (c) Normality Index Map, and (d) Binary Detection Result.

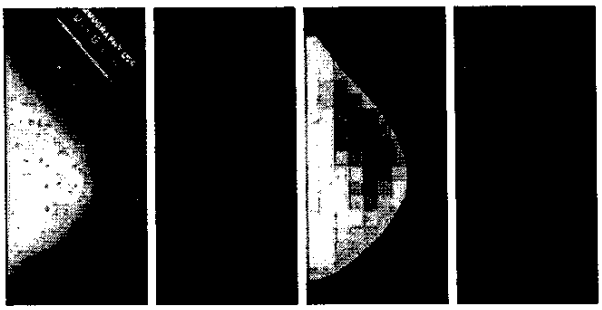

(a) (b) (c) (d)

Figure 5: (a) Whole-Field Mammogram, (b) Residual Image, (c) Normality Index Map, and (d) Binary Detection Result.

set consists of 80 normal and 75 abnormal cases (24 ill-defined or circumscribed masses, 23 spiculated lesions, and 28 microcalcifications). The test set consists of 40 normal and 37 abnormal cases (16 ill-defined or circumscribed masses, 10 spiculated lesion, 11 microcalcifications).

Though this is a normal mammogram classifier, one should keep in mind that the misclassification rate of abnormal mammograms as normal mammograms should be as near zero as possible. It would be risky in mammographic screening if an abnormal is misclassified as normal. Therefore, we set the cost of the misclassification of an abnormal mammogram as a normal one much larger than the cost of the misclassification of a normal case as a suspicious one.

Figure 1 shows the diagram of the normal regional mammogram classifier.

3. DETECTION OF WHOLE-FIELD MAMMOGRAMS

3.1. Breast Region and Background Segmentation

In order to use the normal regional mammogram classifier to classify a whole-field image, the breast region has to be segmented from the background. Otherwise, background noise and artifacts will be classified either as normal or abnormal regions. An automated segmentation algorithm is modified from [11], which is based on histogram thresholding, morphological filtering and boundary shaping.

3.2. Detection Using Several Regions

A moving block scheme is implemented to use the trained binary decision tree in Section 2 on breast regions of segmented whole-field mammograms described above. Each block is 512×512, which is the same size as a ROI used to train the classifier. From Section 2, we know every region is globally labelled either as normal (N) or abnormal (S). Therefore, it is natural to assign every pixel in the block with the same label. The block is then moved every 256 pixels in either direction, resulting in overlapped blocks. Except for the boundary pixels, pixel inside the breast region will be classified in 4 different blocks and be assigned 4, possibly different, labels.

Since each pixel can have four labels associated with it, we need to design a scheme to assign a unique label to each pixel. A Normality Index Map the same size as the whole-field mammogram is introduced to address this problem. First, it is initialized with pixel value 0 for breast tissue and -16 for background pixels. After a moving block is classified, the pixels in the Normality Index Map corresponding to the same position of the current block will be changed by adding -2 if the block is labelled as normal (N), or +2 if the block is labelled abnormal (S). Positive value in the Probability Index Map indicates the high probability of abnormality of the corresponding pixels in the whole-field mammogram. Finally, the Normality Index Map is thresholded to obtain a binary detection image. Figure 2 shows the diagram of the whole-field normality classification.

4. EXPERIMENTAL RESULTS

Figure 3 is the classifier tree that results from the training. Six of 40 testing normal ROIs were misclassified as abnormal, but none of abnormal ROIs were misclassified as normals. We used our approach to classify 35 normal whole field mammograms and 34 abnormal (cancer) whole-field mammograms. The entire breast region of 19 normal cases were classified correctly, and there were only a few small blocks were mislabelled as abnormal in 16 normal cases. There were mainly two types of misclassification: one was due to the edge of bright dense normal tissue; the other was due to the boundary between pectoral muscle and the breast region, which was mostly shown in the MLO view. For the abnormal mammograms, only 17 images had their cancers (including mass, microcalcification and spiculated lesion) correctly identified, and cancers in the other 17 im-

ages were misclassified. However, normal tissue regions were mostly correctly labelled. Figure 4 shows the normal classification of a cancerous mass. The approximate location of the abnormality is highlighted in the final binary detection image. Figure 5 shows the normality classification on a normal mammogram. The final detection image (d) clearly shows it is a normal mammogram.

5. CONCLUSIONS

We obtained fairly satisfactory results from using our new method, though some cancers failed to be identified. One reason was due to the subtlety of some cancers. Another reason was that a tumor needs to be surrounded by the background in the block in order to be classified correctly since abnormal training and testing sets for the decision tree were all of this kind. The advantage of this background-supporting setting is that the bodies of the dense normal areas will not be misclassified as abnormal (mass). Characteristic features need to be further investigated in order to improve the efficiency of the decision tree classifier and reduce the clinically critical misclassification rate of abnormal regions. Meanwhile, this method is being refined and improved toward a sophisticated and clinically sound computer-aided tool for the screening mammography. The detected abnormal regions in Figure 4 (d) may appear inferior to those of computer-aided mass detectors. However, one important issue is that this is a normal mammogram classifier designed to identify all kinds of abnormality, not individual cancer types.

6. REFERENCES

[1] C.J. Vyborny and M.L. Giger, "Computer vision and artificial intelligence in mammography," *American J. of Roentgenology*, vol. 162, no. 3, pp. 699–708, 1994.

[2] S. Liu, C.F. Babbs, and E.J. Delp, "Multiresolution detection of spiculated lesions in digital mammograms," *IEEE Trans. Image Processing*, vol. 10, no. 6, pp. 874–884, June 2001.

[3] J.J. Heine, S. R. Deans, D.K. Cullers, R. Stauduhar, and L.P. Clarke, "Multiresolution statistical analysis of high-resolution digital mammograms," *IEEE Trans. Med. Imag.*, vol. 16, no. 5, pp. 503–515, 1997.

[4] S. Liu, C.F. Babbs, and E.J. Delp, "Normal mammogram analysis and recognition," *Proceedings of the IEEE International Conference on Image Processing*, pp. 727–731, October 4-7 1998.

[5] Y. Sun, C.F. Babbs, and E.J. Delp, "Normal mammogram classifier using binary decision trees on multiresolution features," *Proceedings of the 6th International Workshop on Digital Mammography*, p. Submitted, June 22-25 2002.

[6] M. Heath, K.W. Bowyer, D. Kopans, R. Moore, and Jr. P. Kegelmeyer, "The digital database for screening mammography," *Proceedings of the 5th International Workshop on Digital Mammography*, pp. 212–218, June 11-14 2000.

[7] S. Liu, *The Analysis of Digital Mammograms: Spiculated Tumor Detection and Normal Mammogram Characterization*, Ph.D. Thesis, School of Electrical and Computer Engineering, Purdue University, May 1999.

[8] J. Kovacević and M. Vetterli, "Nonseparable multidimensional perfect reconstruction filter banks and wavelet bases for rn," *IEEE Trans. Inform. Theory*, vol. 38, no. 2, pp. 535–555, March 1992.

[9] S.B. Gelfand, C.S. Ravishankar, and E.J. Delp, "An iterative growing and pruning algorithm for classification tree design," *IEEE Trans. Pattern Anal. Machine Intell.*, vol. 13, pp. 163–174, 1991.

[10] L.Breiman, J.H. Friedman, R.A. Olshen, and C.J. Stone, *Classification and Regression Trees*, Belmont, CA: Wadsworth, 1984.

[11] T. Ojala, J. Näppi, and O. Nevalainen, "Accurate segmentation of the breast region from digitized mammograms," *Computerized Medical Imaging and Graphics*, vol. 25, pp. 47–59, 2001.